Asian Journal of Applied Science and Technology (AJAST)
Volume 7, Issue 2, Pages 23-32, April-June 2023

Identification of Faulting and Structural Styles in the Onshore Fuba field, Niger Delta, Nigeria

U. Ochoma*, I. Tamunobereton-ari, A. R. C. Amakiri, F. B. Sigalo, O. I. Horsfall & O. A. Davies

Department of Physics, Rivers State University, P.M.B 5080, Port Harcourt, Nigeria.
*Corresponding Author (U. Ochoma) - umaocho@gmail.com**

DOI: https://doi.org/10.38177/ajast.2023.7204

Article Received: 22 February 2023 *Article Accepted: 30 March 2023* *Article Published: 29 April 2023*

ABSTRACT

Identification of the faulting and structural styles of Fuba Field, Onshore Niger Delta, Nigeria using Well-logs and 3D Seismic data are here presented. Well-to-Seismic ties, faults and horizon mapping, time-surface generation and depth conversion were carried out using Petrel software. The structural interpretation of seismic data reveal highly synthetic and antithetic faults which are in line with faults trends identified in the Niger Delta. Of the 29 interpreted faults, only synthetic and antithetic faults are regional, running from the top to bottom across the field. These faults play significant roles in trap formation at the upper, middle and lower sections of the field. Two distinct horizons were mapped. Fault and horizon interpretation reveal closures which are collapsed crestal structures bounded by these two major faults. The depth structure maps reveal anticlinal faults. Reservoirs are found at a shallower depth from 6500 to 7500ft and at a deeper depth ranging from 11500 to 13000ft. The synthetic and antithetic faults act as good traps for the hydrocarbon accumulation in the study area. The variance values ranges from 0.0 to 1.0. The Variance edge analysis was used to delineate the prominent and subtle faults in the area. The results from the study will help in the identification of hydrocarbon potentials of the field and also aid in making economic decisions.

Keywords: Growth faults; Horizons; Anticlinal; Structural styles; Variance Method; Niger Delta; Nigeria.

1.0. Introduction

Structural interpretation involves identifying proper geological structures for probable accumulation of hydrocarbon (Majid et al, 2016). Tectonic setting usually governs the structural network and associated features. These traps may be structural, stratigraphic or a combination of both. Majority of traps in the Niger delta are structural (Coffen, 1984; Doust, E. Omatsola, 1990). Structural traps include the faults, anticlines and duplex (Emujakporue and Ngwueke, 2013). Stratigraphic traps include sand channels, pinch-outs, unconformities and other truncations (Folami et al, 2008). In order to get detailed information of the subsurface, petrophysical analysis, reservoir characterization, rock physics analysis, seismic modelling and velocity modelling are indeed essential (Coffen, 1984; Robinson and Coruh, 1988; Lillie, 1991; Dix, 1955).

Several researchers have made enormous contributions based on structural interpretations within the Niger Delta basin to investigate the potentiality of hydrocarbon deposits (Aizebeokhai and Olayinka, 2011; Ameloko and Owoseni, 2015; Horsfall and Ngeri 2019). Aizebeokhai and Olayinka, (2011) delineated horizons and series of growth faults which serve as migratory paths for hydrocarbons into structural closures and reservoir units at large while Ameloko and Owoseni (2015), in their study on hydrocarbon reservoir evaluation of X-field in the Niger Delta using seismic and petrophysical data, deduced from their results on structural interpretations that localized normal faults exist in the study area. Horsfall and Ngeri (2019) delineated horizons and series of faults which is a possible indication that there is a possibility of hydrocarbon accumulation. The northern part forms a large closure against the fault. Some dark stripes were seen on the semblance attribute and shows discontinuities which is synonymous to fault cutting through the seismic time slice, the most inclined fault defines the largest closure which is the prospect zone.

This study is taken from Fuba Field, Depobelt, Niger Delta, Nigeria. The ultimate deliverable of this study was identification of faulting and structural styles of the area. The major components of our study are: (a) Well Correlation performed in order to determine the continuity of the reservoir sand across the field. (b) Seismic Interpretation which involves well-to-seismic ties, fault mapping, horizon mapping, time surface generation, depth conversion, variance attribute generation and structural interpretation.

2.0. Location and Geology of the Study Area

The proposed study area Fuba Field is located in the onshore Niger Delta region. Figure 1 shows the map of the Niger Delta region showing the study area while Figure 2 Schematic Base map showing the study area. The Niger Delta lies between latitudes 4° N and 6° N and longitudes 3° E and 9° E (Whiteman, 1982). The Delta ranks as one of the major oil and gas provinces globally, with an estimated ultimate recovery of 40 billion barrels of oil and 40 trillion cubic feet of gas (Adegoke et al., 2017). The coastal sedimentary basin of Nigeria has been the scene of three depositional cycles (Short and Stable, 1967).

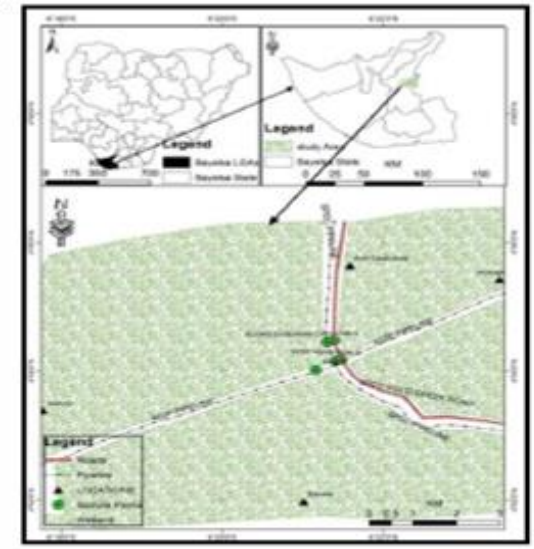

Figure 1. Map of Nigeria Showing The Study Area, Fuba Field

The first began with a marine incursion in the middle Cretaceous and was terminated by a mild folding phase in Santonian time. The second included the growth of a proto-Niger delta during the Late Cretaceous and ended in a major Paleocene marine transgression. The third cycle, from Eocene to Recent, marked the continuous growth of the main Niger delta. A new threefold lithostratigraphic subdivision is introduced for the Niger delta subsurface, comprising an upper sandy Benin Formation, an intervening unit of alternating sandstone and shale named the Agbada Formation, and a lower shaly Akata Formation. These three units extend across the whole delta and each ranges in age from early Tertiary to Recent. They are related to the present outcrops and environments of deposition. A separate member of the Benin Formation is recognized in the Port Harcourt area. It is Miocene-Recent in age with a minimum thickness of more than 6,000ft (1829m) and made up of continental sands and sandstones (>90%) with few shale intercalations (Horsfall et al., 2017). Subsurface structures are described as resulting from movement under the influence of gravity and their distribution is related to growth stages of the delta (Ochoma et al., 2020). Rollover anticlines in front of growth faults form the main objectives of oil exploration, the

hydrocarbons being found in sandstone reservoirs of the Agbada Formation. The oil in geological structures in the basin may be trapped in dip closures or against a synthetic or antithetic fault.

3.0. Methology

3.1. Well-Log and Seismic Data Quality Control

Well correlation involves lithologic description, picking top and base of sand-bodies, fluid discrimination and then linking these properties from one well to another based on similarity in trends. Correlation of reservoir sands was achieved using the top and base of reservoir sands picked. The correlation process was possible based on similarity in the behaviour of the gamma ray log. In the Niger Delta, the predominant lithologies are sands and shales. In order to discriminate between these two lithologies in the subsurface, the gamma ray log is used. After defining the lithologies, the resistivity log was used for discriminating the type of fluid occurring within the pores in the rocks.

There are seven basic steps involved in seismic interpretation relevant to this study and they include well-to-seismic ties, Fault Mapping, Horizon mapping, Time surface generation, velocity Modelling, Depth Conversion and generation of variance attribute. The sonic log, which is the reciprocal of velocity, was calibrated using the checkshot data. The calibration process is necessary in order to improve the quality of the sonic log because the sonic log is prone to washouts and other wellbore related issues. The results of calibrating the sonic log with the checkshot gives the calibrated sonic log.

The calibrated sonic log is used along with the density log to generate an acoustic impedance (AI) log. The acoustic impedance log is calculated for each layer of rock. The next step involves generating the reflectivity coefficient (RC) log. The RC is calculated and generated using the AI log. The RC log generated is then convolved with a wavelet to generate a synthetic seismogram which is comparable with the seismic data. The statistical wavelet utilized for convolution is extracted from the seismic data. The synthetic seismogram was generated. The mathematical expressions that govern the entire well-to-seismic tie workflow are presented below:

$$AI = \rho v \qquad (1)$$

$$RC = \frac{\rho_2 v_2 - \rho_1 v_1}{\rho_2 v_2 + \rho_1 v_1} \qquad (2)$$

$$\text{Synthetic Seismogram} = \frac{\rho_2 v_2 - \rho_1 v_1}{\rho_2 v_2 + \rho_1 v_1} * wavelet \qquad (3)$$

where AI = acoustic impedance, RC = reflection coefficient, ρ = density; v = velocity.

Faults were identified as discontinuities or breaks in the seismic reflections. Faults were mapped on both inline and cross-line directions. Horizons are continuous lateral reflection events that are truncated by fault lines. The horizon interpretation process was conducted along both inline and crossline direction. At the end of the horizon mapping, a seed grid is generated which serves as an input for time surface generation. Time surfaces were generated using the seed grids gotten from the horizon mapping process. The third order polynomial velocity model generated was used to depth convert the time surfaces of the reservoirs of interest.

3.2. Variance (Edge Detection) Method

The variance attribute is edge imaging and detection techniques. It is used for imaging discontinuity related to faulting or stratigraphy in seismic data. Variance attribute is proven to help in imaging of channels, fault zones, fractures, unconformities and the major sequence boundaries (Pigott. et al, 2013). In the Petrel software, the variance attribute uses an algorithm that computes the local variance of the seismic data through a multi-trace window with user-defined size. The local variance is computed from horizontal sub-slices for each voxel. A vertical window was used for smoothing the computed variance and the observed amplitude normalized. The variance attribute measures the horizontal continuity of the amplitude that is the amplitude difference of the individual traces from their mean value within a gliding CMP window.

$$\sigma^2 = \frac{1}{n}\sum_{f_i=1}^{n}(x_i + x_m)^2 \qquad (4)$$

Where $\sigma =$ standard deviation, $\sigma^2 =$ variance, $n =$ the number of observations, $f_i =$ frequency, $x_i =$ the variable, $x_m =$ mean of x_i

4.0. Results and Discussion

4.1. Reservoir Identification, Correlation and Well-to-Seismic Ties

The results for lithology and reservoir identification are presented in (Figure 2). A total of nine sand bodies (A, B, C, D, E, F, G, H, I) were identified and correlated across all seven wells in the field. Two reservoir sands were selected for the purpose of this study (A and I). The resistivity logs which reveals the presence of hydrocarbons were used to identify the hydrocarbon bearing sands. On (Figure 2), the sands are coloured yellow while shales are grey in colour. The results for well-to-seismic tie conducted on Fuba field using density log, sonic log and checkshot of Well-1 is presented in Figure 3. A statistical wavelet (ISIS time) was used to give a near perfect match between the seismic and synthetic seismogram.

4.2. Faults and Horizons Interpretation

The results for the interpreted faults in Fuba field are presented in Figure 4 shows both synthetic and antithetic faults interpreted along seismic inlines. Faults are more visible along the inline direction because this direction reveals the true dip position of geologic structures. The variance time slice was used to validate the interpreted faults as seen on Figure 5. All interpreted faults are normal synthetic and antithetic faults. A total of twenty-nine faults were interpreted across the entire seismic data. Of the 29 interpreted faults, only F1 (synthetic fault) and F16 (antithetic fault) faults are regional, running from the top to bottom across the field. Hence, these faults play significant roles in trap formation at the upper, middle and lower sections of the field. As can be seen from Figure 6, all drilled wells within the field are within the two major faults identified (F1 and F16 faults).

The results for the interpreted seismic horizons (Horizon A and Horizon I) are also presented in Figure 4. On these horizons, the fault polygons were generated and eliminated. The horizons were used as inputs for the generation of reservoir time surfaces. The reservoir time surfaces (A and I reservoirs) reveal that the reservoir structure is a

collapsed crest, bounded by two regional faults (F1 and F16). Reservoirs A and I time surfaces are truncated by two bounding faults and three minor inter-reservoir faults. The similarity in structure identified on reservoirs A and I reveals that the field is structurally controlled by faults.

4.3. Depth Surfaces

The result of depth conversion residual analysis is presented in Table 1. The depth residual is the difference between the depth values of the well top from each well and the depth value from the depth converted reservoir surfaces. The depth residual analysis revealed that surfaces converted using the linear velocity function had the largest residuals ranging from -31.60 to +61.67 and from -50.58 to +40.84ft in reservoir A and reservoir I respectively. This is closely followed by the residual values obtained with the 2nd order polynomial function.

The third order polynomial function shows the least residuals, ranging from -6.69 to +6.61 ft in reservoir A, and -9.48 to +8.42ft respectively. The negative depth residual indicates that the depth conversion process displaces the reservoir to a greater depth than where it occurs in the subsurface, while a positive depth residual signifies that the depth converted result has placed the reservoir at a shallower depth (Ogbamikhumi and Aderibigbe, 2019). The resultant depth residual values generated using the various velocity models (linear, 2nd and 3rd order polynomials) were compared in order to select the most suitable velocity model for depth conversion of the reservoir surfaces. Figure 7 shows the 3rd order polynomial velocity model which was selected and used as most suitable velocity model for converting A and I reservoirs from time to depth because it has the least residuals.

The depth converted reservoir A and I surfaces are presented in Figures 8 and 9 for the third order polynomial velocity function. The depth structure maps reveal that the reservoirs are anticlinal and fault supported. Reservoir A is found at a shallower depth from 6500 to 7500 ft while reservoir I is found at a deeper depth ranging from 11500 to 13000ft respectively. The depth residuals recorded from the various well locations were used to generate depth residual maps which are presented in Figures 10 and 11 respectively. The depth residual maps revealed that higher residuals on reservoir A and I surfaces are associated with the eastern and western regions which are areas not penetrated by any well.

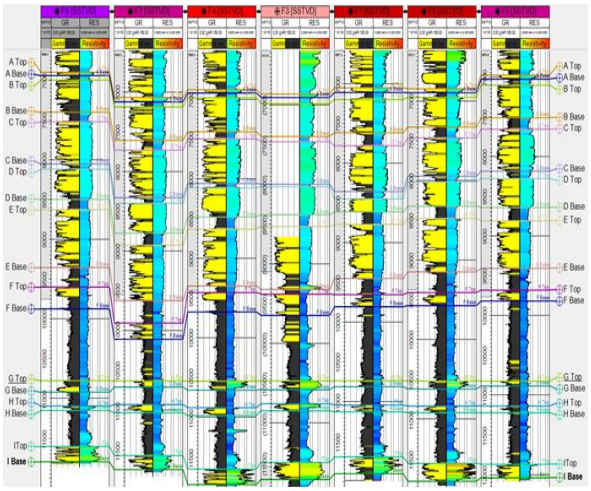

Figure 2. Well Section Showing Reservoir Identified and Correlated Across Fuba Field

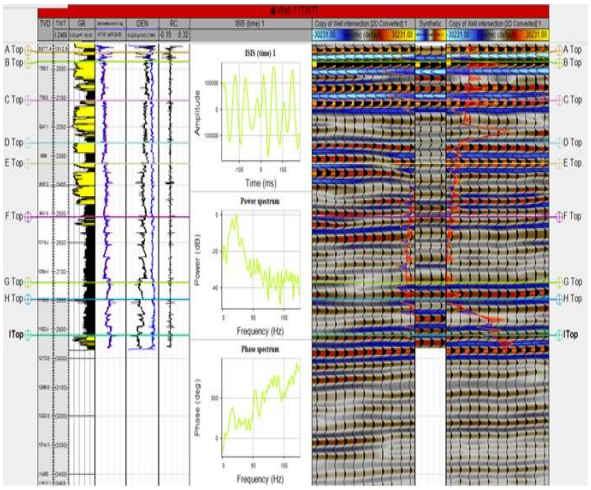

Figure 3. Synthetic Seismogram Generation and Well-to-seismic Tie Conducted for Fuba Field using Well-1

Asian Journal of Applied Science and Technology (AJAST)
Volume 7, Issue 2, Pages 23-32, April-June 2023

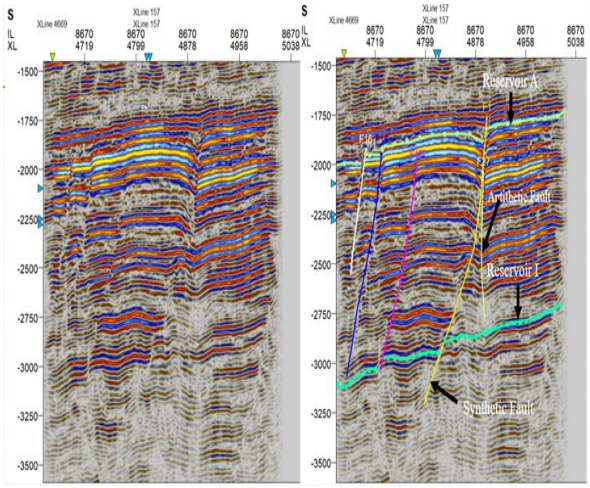

Figure 4. Faults and Horizons Interpreted Along Seismic Inline section (a) Original Seismic, (b) Faults and Horizons Interpreted

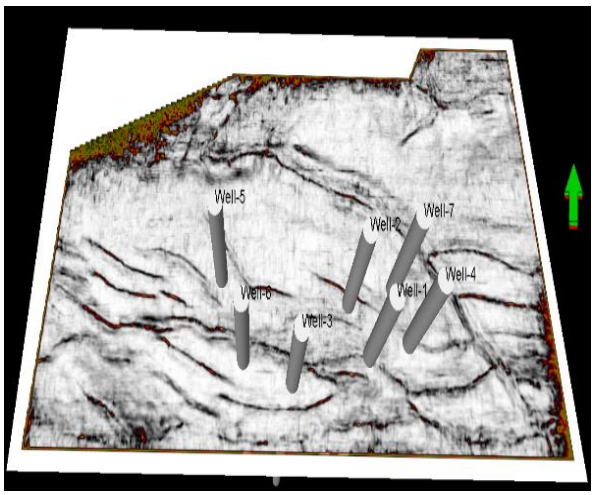

Figure 5. Variance Attribute Generated Showing Clearly Resolved Faults on Time Slice

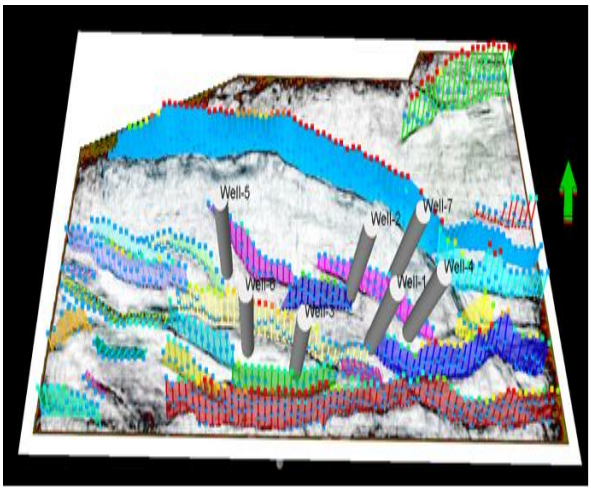

Figure 6. Interpreted Faults Displayed on the Variance Time Slice

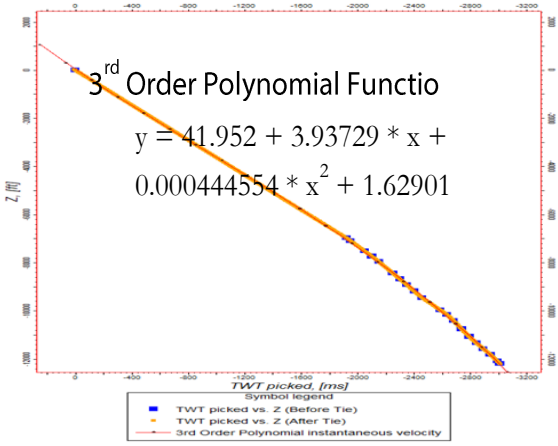

Figure 7. Third Order Polynomial Velocity model Utilized for Converting Reservoir Surfaces from Time to Depth

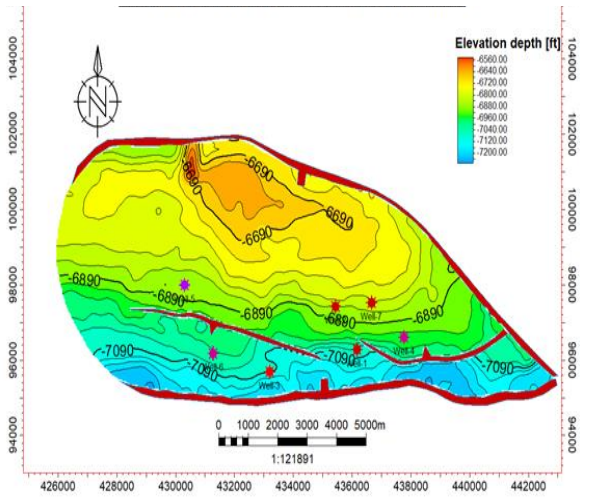

Figure 8. Depth Converted Reservoir Surfaces Using the 3rd Order Polynomial Velocity Function for Reservoir A

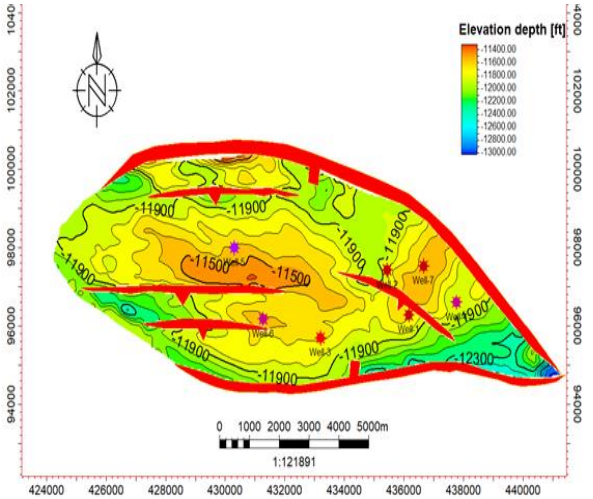

Figure 9. Depth Converted Reservoir Surfaces Using the 3rd Order Polynomial Velocity Function for Reservoir I

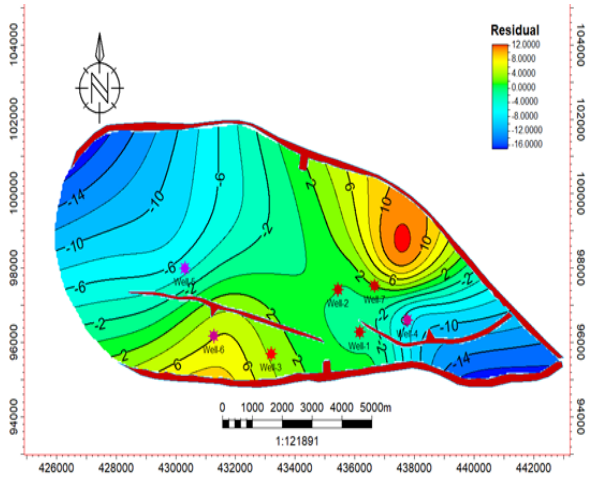

Figure 10. Depth Residual Maps Generated from Surfaces Converted Using the 3rd Order Polynomial Velocity Function for Reservoir A

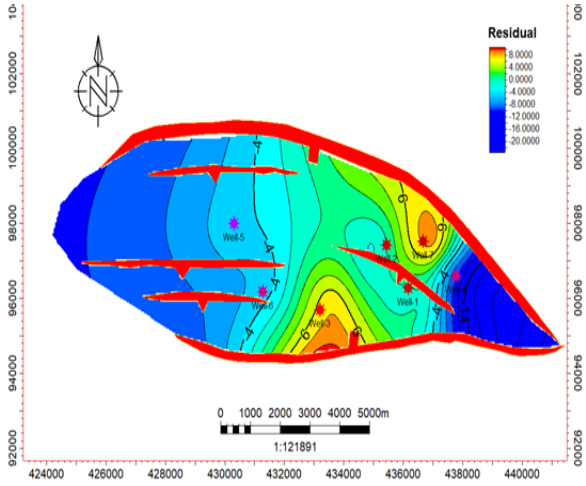

Figure 11. Depth Residual Maps Generated from Surfaces Using the 3rd Order Polynomial Velocity Function for Reservoir I

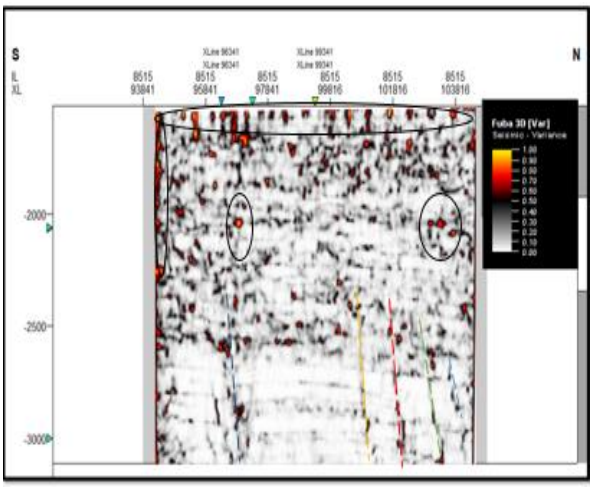

Figure 12. Variance Edge inline 8515

4.4. Variance (Edge Detection) Method

Figure 12 shows the computed variance attributes of the seismic section. The variance values range from 0.0 to 1.0. Values of variance equal to 1 represent discontinuities while a continuous seismic event is represented by the value of 0. The high values are denoted with red to yellow colorations.

On the variance map, the areas dotted with blue, green, orange and pink colored lines signify values that correspond to the location of the discontinuity. The discontinuities may be interpreted as faults and boundaries as shown by the lines drawn on the variance attribute map (Law and Chung, 2006). The variance edge enhanced the faults or sedimentological bodies within the seismic data volume. Furthermore, several bright spots are also delineated (in black circles and black ovals) which indicate high reflectivity sediments compared to their surroundings.

These bright spots are an indication that a potential hydrocarbon trap might exist in the area. The darkest regions in the seismic section, which make vertical strips, may be interpreted as faults or fractures. The zones with low variance values are due to similar seismic traces. Areas with red patches represent lineaments/discontinuities while grey areas represent the structural framework of the field.

Table 1. Depth Residual between Well Tops and Resultant Depth Surfaces

Reservoir/Well	Well Top (ft)	Depth Surface (ft)	Difference (ft)	Depth Surface (ft)	Difference (ft)	Depth Surface (ft)	Difference (ft)
		Linear Velocity Function		*2nd Order Polynomial*		*3rd Order Polynomial*	
Reservoir A Well-1	-7054.07	-7079.08	25.01	-7032.58	-21.49	-7053.13	-0.95
Well-2	Missing	Missing	Missing	Missing	Missing	Missing	Missing
Well-3	-6877.06	-6849.08	-27.98	-6886.40	9.34	-6880.86	3.80
Well-4	-6977.93	-7039.60	61.67	-7004.73	26.80	-6971.24	-6.69
Well-5	-6905.39	-6873.79	-31.60	-6859.58	-45.81	-6900.65	-4.74
Well-6	-7065.18	-7105.10	39.92	-7028.91	-36.27	-7070.87	5.69
Well-7	-6846.24	-6877.44	31.20	-6854.65	8.41	-6852.85	6.61
Reservoir I Well-1	-11690.91	-11720.12	29.21	-11674.22	-16.69	-11690.91	0.00
Well-2	-11823.41	-11780.54	-42.87	-11807.54	-15.87	-11823.41	0.00
Well-3	-11650.06	-11684.44	34.38	-11666.36	16.30	-11656.67	6.61
Well-4	-11887.08	-11845.26	-41.82	-11912.42	25.34	-11877.60	-9.48
Well-5	-11599.86	-11549.01	-50.85	-11581.29	-18.57	-11595.11	-4.75
Well-6	-11569.00	-11534.94	-34.06	-11586.60	17.60	-11564.27	-4.73
Well-7	-11551.91	-11592.75	40.84	-11534.64	-17.27	-11560.33	8.42

5.0. Conclusion

A total of nine sand bodies (A, B, C, D, E, F, G, H, I) were identified and correlated across all seven wells in the field. Two horizons (A and I) were selected for the study. Structural analysis of the field revealed that reservoir A and I are anticlinal structures supported by two major bounding faults. Structural interpretation of seismic data revealed that the field is highly faulted with synthetic and antithetic faults which are in line with faults trends identified in the Niger Delta. All interpreted faults are normal synthetic and antithetic faults. A total of twenty-nine faults were interpreted across the entire seismic data. Of the 29 interpreted faults, only F1 (synthetic fault) and F16 (antithetic fault) faults are regional, running from the top to bottom across the field. Hence, these faults play significant roles in trap formation at the upper, middle and lower sections of the field. Fault and horizon interpretation revealed that closures found on A and I reservoirs are collapsed crestal structures bounded by the two

major faults. The depth structure maps reveal that the reservoirs are anticlinal and fault supported. Reservoir A is found at a shallower depth from 6500 to 7500ft while reservoir I is found at a deeper depth ranging from 11500 to 13000ft respectively. The synthetic and antithetic faults act as good traps for the hydrocarbon accumulation in the study area. The variance map revealed the subtle structures and faults in the seismic section. The variance attribute analysis in this study has helped in increasing the understanding of the delineated reservoirs and geological structures in the study area towards a better delineation of hydrocarbon potential and improved reservoir characterization. Furthermore, it has been demonstrated that seismic attributes are complementary to the information derived through traditional methods of seismic interpretation. In reservoirs, hydrocarbons were encountered by all seven wells drilled in the field.

Declarations

Source of Funding

This study did not receive any grant from funding agencies in the public or not-for-profit sectors.

Competing Interests Statement

Authors have declared no competing interests.

Consent for Publication

The authors declare that they consented to the publication of this study.

Acknowledgments

The authors are grateful to Shell Petroleum Development Company of Nigeria (SPDC), Port Harcourt Nigeria for the release of the academic data for the purpose of this study.

References

[1] Adegoke, O.S., Oyebamiji, A.S., Edet, J.J., Osterloff, P.L. & Ulu, O.K. (2017). Cenozoic foraminifera and calcareous nannofossil biostratigraphy of the Niger Delta. Elsevier, Cathleen Sether, United States.

[2] Aizebeokhai, A.P. & Olayinka, I. (2011). Structural and Stratigraphic Mapping of EMI Field, Offshore Niger Delta. Journal of Geology and Mining, 3(2): 25–38.

[3] Ameloko, A.A. & Owoseni, A.M. (2015). Hydrocarbon Reservoir Evaluation of X-field, Niger Delta Using Seismic and Petrophysical Data. International Journal of Innovation and Scientific Research, 15(1): 193–201.

[4] Coffen, J.A. (1984). Interpreting Seismic Data. Penwell Publishing Company, Tusla, Oklahoma, Pages 39–118.

[5] Coffeen J.A. (1984). Seismic Exploration Fundamentals. Penwell Publication Company.

[6] Doust, H. & Omatsola, E. (1990). Niger Delta Margin Basins. AAPG Memoir, 48: 239–248

[7] Dix, C.H. (1955). Seismic velocity from surface measurements. Geophysics, 20: 68–86.

[8] Emujakporue G.O. & Ngwueke, M.I. (2013). Structural Interpretation of Seismic Data from an xy Field, onshore Niger Delta, Nigeria. Journal of Applied Sciences and Environmental Management, 17(1): 153–158.

[9] Folami, T.O., Ayuk, M.A. & Adesida, A. (2008). Identification of Hydrocarbon Reservoirs Using Seismic Attributes and Geocellular Modelling: A Case Study from "Tyke" Field, Niger Delta, Nigeria. Association of Petroleum Geologists Bulletin, Pages 30–32.

[10] Horsfall, O.I. & Ngeri A.P. (2019). Structural Interpretation of AKOS Field, Coastal Swamp Depobelt, Niger Delta, Nigeria. Asian Journal of Applied science and Technology (AJAST), 3(1): 68–77.

[11] Horsfall, O.I., Uko, E.D., Tamunoberetonari I., & Omubo-Pepple, V.B. (2017). Rock-Physics and Seismic-Inversion Based Reservoir Characterization of AKOS FIELD, Coastal Swamp Depobelt, Niger Delta, Nigeria. IOSR Journal of Applied Geology and Geophysics, 5(4): 59–67.

[12] Law W.K. & Chung A.S.C. (2006). Minimal Weighted Local Variance as Edge detector for Active Contour Models. In: Narayanan et al. PJ (eds), LNCS 3851, Pages 622–632.

[13] Lillie, R. (1991). Whole Earth Geophysics: An Introductory Textbook for Geologists and Geophysicist. PH.

[14] Majid, K., Shahid, N., Munawar, S & Muhammad, H. (2016). Interpreting Seismic Profiles in Terms of Structure and Stratigraphy with Implications for Hydrocarbons Accumulation, an Example from Lower Indus Basin Pakistan. Journal of Geology and Geophysics, 5(5): 257.

[15] Robinson, E.S. & Coruh, C. (1988). Basic Exploration Geophysics. Wiley.

[16] Ochoma, U., E.D. Uko, E.D. & Horsfall, O.I. (2020). Deterministic Hydrocarbon Volume Estimation of the Onshore Fuba Field, Niger Delta, Nigeria. IOSR Journal of Applied Geology and Geophysics, 8(1): 34–40.

[17] Ogbamikhumi, A. & Aderibigbe, T.O. (2019). Velocity modelling and depth conversion uncertainty analysis of onshore reservoirs in the Niger Delta basin. Journal of the Cameroon Academy of Sciences, 14(3): 239–247.

[18] Pigott J.D., Kang, M.I.H. & Han, H.C. (2013). First Order Seismic Attributes for Clastic Seismic Facies Interpretation: Examples from the East China Sea. Journal of Asian Earth Science, 66: 34–54.

[19] Short, K.C. & Stable, A.J. (1967). Outline of Geology of Niger Delta. Bulletin of America Association of Petroleum Geologists, 51(5): 761–779.

[20] Whiteman, A. (1982). Nigeria: Its Petroleum Ecology Resources and Potential, Graham and Trotman, London.